Bone Laminarity in the Avian Forelimb Skeleton and Its Relationship to Flight Mode: Testing Functional Interpretations

ERIN L.R. SIMONS[1]* AND PATRICK M. O'CONNOR[2]
[1]Department of Anatomy, Midwestern University, Glendale, Arizona
[2]Department of Biomedical Sciences, Ohio University, Athens, Ohio

ABSTRACT

Wing bone histology in three species of birds was characterized in order to test hypotheses related to the relationship between skeletal microstructure and inferred wing loading during flight. Data on the degree of laminarity (the proportion of circular vascular canals) and the occurrence of secondary osteons were obtained from three species that utilize different primary flight modes: the Double-crested cormorant, a continuous flapper; the Brown pelican, a static soarer; and the Laysan albatross, a dynamic soarer. Laminarity indices were calculated for four quadrants for each of the three main wing elements. Ulnae and carpometacarpi were predicted to exhibit quadrant specific patterns of laminarity due to hypothesized differences in locally applied loads related to the attachment of flight feathers. However, few differences among the quadrants were identified. No significant differences were identified among the three elements, which is notable as different bones are likely experiencing different loading conditions. These results do not support the concept of bone functional adaptation in the primary structure of the wing elements. Significant differences in laminarity were found among the three primary flight modes. The dynamic soaring birds exhibited significantly lower laminarity than the flapping and static soaring birds. These results support the proposed hypothesis that laminarity is an adaptation for resisting torsional loading. This may be explained by overall wing shape: whereas dynamic soaring birds have long slender wings, flappers and static soaring birds have broader wings with a larger wing chord that would necessarily impart a higher torsional moment on the feather-bearing bones. Anat Rec, 295:386–396, 2012. © 2012 Wiley Periodicals, Inc.

Key words: bone microstructure; bone histology; bone biomechanics; laminarity; flight mode

Additional Supporting Information may be found in the online version of this article.

Grant sponsors: Ohio University Graduate Student Senate, the Ohio University Office of Research and Sponsored Programs (ELRS), the Ohio University Heritage College of Osteopathic Medicine (PMO).

*Correspondence to: Erin Simons, Department of Anatomy, Midwestern University, 19555 North 59th Ave, Glendale, AZ 85308. E-mail: esimon@midwestern.edu

Received 9 August 2011; Accepted 26 November 2011.
DOI 10.1002/ar.22402
Published online 12 January 2012 in Wiley Online Library (wileyonlinelibrary.com).

INTRODUCTION

The majority of avian cortical bone retains its primary structure and is not remodeled throughout life to the extent observed in most mammals (Enlow and Brown, 1957; Currey, 1960). In general terms avian cortex consists of a densely vascularized fibro-lamellar complex (de Ricqlés et al., 1991). Bone microstructure is organized such that primary osteons are arranged around vascular canals, with these bone-vascular units (BVUs) exhibiting a combination of longitudinal, radial, circular, and oblique orientations (Enlow and Brown, 1957; de Ricqlés et al., 1991; de Margerie, 2002). These four categories of primary vascular structure were summarized by de Ricqlés et al. (1991) and can be defined as follows: (1) longitudinal canals run parallel to the long axis of the bone (and thus appear circular in cross section; Fig. 1); (2) radial canals lie in the plane of a cross section and are oriented normal to the external surface of the bone, (3) circular canals also lie in the plane of a cross section and are oriented parallel to the external surface of the bone, and (4) oblique canals are oriented in directions other than (1) through (3) defined above (de Ricqlés et al., 1991; de Margerie, 2002). Primary bone may have a combination of these four vascular canal orientations. Bone with a predominance of circular canals is defined as laminar bone; bone organization consisting of primarily oblique canals is termed reticular (de Ricqlés et al., 1991; de Margerie, 2002).

Differences in vascular canal orientation may reflect differences in growth rate, phylogeny, or function, with all being proposed as primary determinants of bone microstructure at some point over the past 120 years (Wolff, 1892; Amprino, 1947; Castanet et al., 2000; de Margerie, 2002; de Margerie et al., 2002; Skedros et al., 2003). Recent studies examining the relationship of vascular canal orientation and bone growth in birds reveal conflicting interpretations as to the linkage between these two variables. For example, it has been documented that (1) the highest rates (up to 171 μm/day) of bone deposition were associated with radially oriented canal organization (de Margerie et al., 2004), (2) the highest rates (up to 80 μm/day) were associated with reticular and laminar canal organization (Castanet et al., 2000), (3) that the rates of deposition of different canal organizations were equivalent (de Margerie et al., 2002), and (4) that the same canal organization (longitudinal) was produced by a range (10–50 μm/day) of growth rates (Starck and Chinsamy, 2002). Such seemingly contradictory results related to the effect of growth rate on bone deposition (and hence, bone microstructural patterning) in birds suggest that other factors such as the possible phylogenetic or functional influences must also be considered (de Margerie et al, 2002, 2004). Note: these studies are only marginally comparable, having been conducted on a range of elements in different taxa under different testing conditions; nonetheless, interpretations from these studies have formed the basis for inferences about the microanatomical form-function relationships in birds more generally (e.g., de Margerie et al., 2005).

As one example, a predominance of circular canals in bone (forming a laminar structure) has been hypothesized to represent a structural adaptation for resisting high torsional loads (i.e., interpreted as shear loading at the tissue level) (de Margerie, 2002; Skedros and Hunt, 2004; de Margerie et al., 2005). In particular, specific bones (humeri, ulnae) of the avian skeleton either hypothesized (Pennycuick, 1967) or known (see Biewener and Dial, 1995) to experience torsional loading associated with flapping flight tend to exhibit highly laminar bone structure (de Margerie, 2002; Skedros and Hunt, 2004; de Margerie et al., 2005). de Margerie (2002) developed a method to quantify the amount of laminar bone present in a bone section (the degree of laminarity). In this method the number of each type of canal (longitudinal, radial, circular, or oblique) is tallied and a Laminarity Index is calculated (LI = total # circular canals/total # canals). This method has been used to describe differences in microstructure within a bone section due to localized loads caused by flight feather attachment to the ulna (Skedros and Hunt, 2004), as well as more generally among a broad survey of birds to reveal patterns of variation in the degree of laminarity that may correspond to overall wing shape and flight behavior (de Margerie et al., 2005).

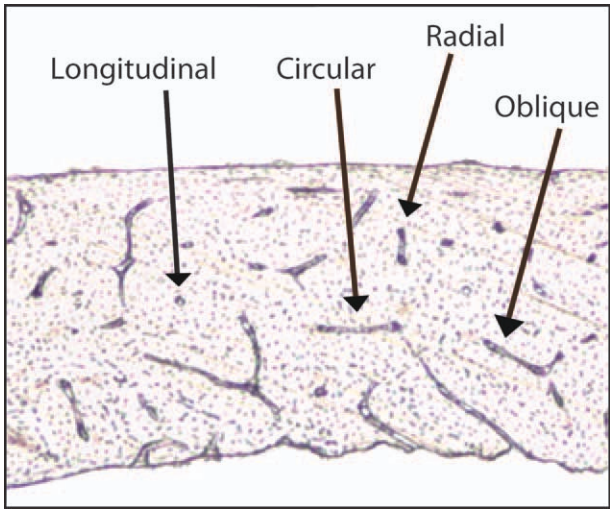

Fig. 1. Examples of the four types (longitudinal, circular, radial, and oblique) of primary vascular canal orientations in a Double-crested cormorant (*Phalacrocorax auritus*, OUVC 10431).

The degree of laminarity in bone tissue has also been found to be positively correlated with cortical thickness, cross-sectional shape and collagen fiber orientation. Using basic beam mechanics, de Margerie et al. (2005) examined avian long bones and identified a more circular cross-section, in conjunction with relatively less material (i.e., thinner cortices) positioned distantly from the neutral axis, as consistent with general interpretations that this configuration is optimized to resist torsional loading. They also noted increasing birefringence (i.e., oblique-to-transverse arrays) of collagen under circularly polarized light microscopy, and this, together with the spatial characteristics noted above, was strongly correlated with the highest degree of laminarity. Notably these correlations were strongest among humeri, ulnae, and femora, all of which are hypothesized to experience primarily torsional loads during normal activities. This puts in place a strong functional argument that we can now test using a flight-mode diverse

(and thus, biomechanical-load-variable) assemblage of birds.

Pelecaniforms, along with other neoavian seabirds (e.g., procellariiforms), include taxa that utilize a diverse array of primary flight modes, ranging from those that perform continuous flapping to stay aloft to others that use energy-saving techniques such as soaring and gliding (Johnsgard, 1993; Tickell, 2000; Nelson, 2005). Different primary flight modes no doubt induce different loading conditions (e.g., frequency, magnitude, orientation of loads) on the forelimb skeleton, and the physical manifestations of the loading environment may in turn be reflected in the bony organization of the individual wing elements (e.g., Simons, 2010; Simons et al., 2011). For example, in their recent study of pelecaniform birds Simons et al. (2011) examined bone cross-sectional geometry in the context of flight style variability (e.g., flapping vs. soaring) and demonstrated that birds utilizing soaring as a primary flight mode exhibit wing bone cross-sections optimized to resist torsional loads (i.e., thin-walled, circular cross-sections, etc.). Not only do such traits manifest at the bone level in the form of the cross-sectional shape and the distribution of bone tissue, but given the context provided by de Margerie et al. (2005) on laminarity, we predict that differential flight mode (and hence, inferred loading differences) would also impact microstructural organization (i.e., degree of laminarity) and can be used to test structural hypotheses such as that proposed for primary bony architecture.

In this study we assessed the degree of laminarity in the three main wing elements (humerus, ulna, and carpometacarpus) of three species of birds that utilize different primary flight modes. We investigated whether the hypothesized loading patterns of these elements are related to differences in the structure of the bone at the tissue level. We addressed three main questions. Question 1—Are there differences in the degree of laminarity among the main quadrants of each element (dorsal, cranial, ventral, caudal)? We predict that within the ulna and carpometacarpus, the attachment of flight feathers induce local loads that may affect the microstructural orientation in the dorsal part of the section (see Skedros and Hunt, 2004). In addition, a bending load, such as that predicted to occur in the carpometacarpus, imparts local tension and compression on different parts of the element, which may in turn affect the microstructure (Simons et al., 2011). Question 2—Are there differences in the degree of laminarity among the three elements? We predict that the humerus (proximal element) exhibits higher laminarity (LI) than more distal elements. Previous studies have shown that the humerus exhibits a cross-sectional shape that is optimized to resist torsion relative to more distal elements (Simons et al., 2011). Question 3—Are there differences in the degree of laminarity among birds that utilize different primary flight modes? We predict that the forelimb elements of birds that utilize static soaring will exhibit higher LI than those of birds utilizing other flight modes, based on the large, broad wing of static soaring birds relative to birds utilizing other flight modes (Simons et al., 2011). In addition, although avian bone is predominantly primary in nature, some secondary (Haversian) remodeling does occur (Enlow and Brown, 1957; Currey, 1960). We therefore noted the presence and location of secondary (Haversian) osteons within the examined elements.

MATERIALS AND METHODS

In this study we extensively sampled three species of bird: Brown pelican (*Pelecanus occidentalis*), Double-crested cormorant (*Phalacrocorax auritus*), and Laysan albatross (*Phoebastria immutabilis*). These three focal taxa were explicitly chosen based on both functional and phylogenetic grounds, allowing us to contrast both flight mode and familial comparisons in the study (Table 1). Moreover, we were able to sample the appropriate number of individuals of the three species necessary for assessing intraspecific variation, a seldom accomplished goal in studies of this nature. We collected histological samples from six skeletally mature individuals of each species. As noted above, each species represents a form that uses a different primary flight mode. The static soaring Brown pelican and continuous flapping Double-crested cormorant, both pelecaniform birds, represent a within clade comparison of flight mode variability. In addition, the dynamic soaring procellariiform is used as a contrast with the pelecaniform taxa. We also sampled two specimens each of two other taxa, the dynamic soaring Northern gannet (*Morus bassanus*, a pelecaniform bird) and the static soaring Red-tailed hawk (*Buteo jamaicensis*, a falconiform bird). Data from these additional taxa were not used in statistical analyses and only used for comparative purposes. Birds used in this study were salvage specimens obtained from rehabilitation centers and were preserved frozen prior to histological sampling. Skeletal maturity was assessed based on the presence of adult plumage patterns. Although all specimens included in this study were adults, the specific ages of the individuals were unknown. All birds used in this study are reposited in the Ohio University Vertebrate Collections (OUVC, see Table 1 for accession numbers). Histological samples along with digital copies of the entire cross section are on file with the corresponding author.

Histological Preparation

The three main elements (humerus, ulna, and carpometacarpus) were removed from the right-side wing of each specimen. After the total length of each element was measured, a 3–4 cm segment of the midshaft of each element was excised. Bones were sampled at midshaft to avoid localized effects of muscle attachments and because the maximum stress is predicted to occur at mid-shaft (Beer et al., 2006). A fine-tipped permanent ink pen was used to mark a "v" on the ventral surface of each segment, with the apex of the "v" pointing distally such that it could be used as a guide for orienting and maintaining segments during the embedding process. The excised bone segments were fixed in formalin (10% buffered neutral) for 24 hr and dehydrated in a graded ethanol series (70, 80, 95, and 100%; changed every 24 hr, 2 changes of each) following protocols outlined in An and Martin (2003). The three segments from each individual were embedded using Epo-Thin (Buehler) low viscosity epoxy, making sure orientation (both proximal–distal and dorsoventral–craniocaudal) was consistent. Subsequent to polymerization ($\sim$ 12 hr on average), a 1 mm thick section was cut from each block using a Buehler IsoMet® 1000 Precision Saw and IsoCut® Plus cutting fluid (Buehler). Sections were mounted to a

TABLE 1. Laminarity index (LI) for each quadrant for each element from all specimens used in study

		LI Humerus				LI Ulna				LI Carpometacarpus			
UVC#	Species	Dorsal	Cranial	Ventral	Caudal	Dorsal	Cranial	Ventral	Caudal	Dorsal	Cranial	Ventral	Caudal
10,437	Double-crested cormorant	0.18	0.30	0.16	0.09	0.26	0.15	0.31	0.12	0.03	0.45	0.14	0.09
10,479	Double-crested cormorant	0.69	0.50	0.25	0.43	0.64	0.37	0.50	0.32	0.29	0.42	0.12	0.51
10,482	Double-crested cormorant	0.51	0.41	0.29	0.34	0.59	0.15	0.41	0.25	0.23	0.41	0.42	0.36
10,436	Double-crested cormorant	0.39	0.52	0.19	0.44	0.23	0.11	0.00	0.12	0.18	0.32	0.13	0.43
10,505	Double-crested cormorant	0.67	0.28	0.16	0.15	0.19	0.14	0.26	0.00	0.19	0.25	0.21	0.10
10,431	Double-crested cormorant	0.31	0.49	0.12	0.30	0.38	0.33	0.40	0.51	0.14	0.26	0.12	0.17
10,478	Brown pelican	0.50	0.70	0.23	0.80	0.00	0.30	0.60	0.21	0.55	0.11	0.33	0.00
10,484	Brown pelican	0.46	0.44	0.60	0.43	0.12	0.46	0.44	0.31	0.60	0.09	0.25	0.29
10,494	Brown pelican	0.56	0.23	0.29	0.40	0.32	0.64	0.30	0.57	0.35	0.07	0.26	0.11
10,433	Brown pelican	0.65	0.09	0.09	0.35	0.50	0.05	0.31	0.32	0.25	0.00	0.04	0.19
10,440	Brown pelican	0.63	0.62	0.13	0.76	0.59	0.38	0.83	0.45	0.28	0.21	0.33	0.40
10,430	Brown pelican	0.68	0.23	0.19	0.50	0.12	0.38	0.26	0.43	0.44	0.18	0.39	0.44
10,480	Laysan albatross	0.16	0.07	0.09	0.15	0.00	0.16	0.13	0.03	0.04	0.08	0.03	0.03
10,481	Laysan albatross	0.00	0.03	0.13	0.17	0.04	0.03	0.00	0.06	0.06	0.16	0.07	0.26
10,483	Laysan albatross	0.10	0.07	0.12	0.08	0.00	0.03	0.06	0.00	0.09	0.00	0.06	0.06
10,439	Laysan albatross	0.09	0.19	0.05	0.23	0.07	0.08	0.00	0.18	0.05	0.00	0.00	0.09
10,509	Laysan albatross	0.13	0.06	0.06	0.26	0.13	0.16	0.09	0.06	0.15	0.23	0.16	0.17
10,225	Laysan albatross	0.07	0.03	0.00	0.03	0.00	0.02	0.03	0.06	0.08	0.07	0.00	0.15
10,434	Northern gannet*	0.32	0.17	0.08	0.00	0.04	0.00	0.00	0.00	0.00	0.00	0.00	0.00
10,492	Northern gannet*	0.47	0.18	0.07	0.05	0.08	0.00	0.08	0.03	0.09	0.00	0.03	0.00
10,506	Red-tailed hawk*	0.78	0.75	0.71	0.56	0.65	0.53	0.68	0.50	0.43	0.62	0.76	0.37
10,507	Red-tailed hawk*	0.88	0.69	0.55	0.73	0.41	0.33	0.85	0.73	0.23	0.47	0.55	0.67

Shaded values indicate quadrants in which secondary remodeling was present. Asterisk (*) indicates specimens not included in statistical analysis.

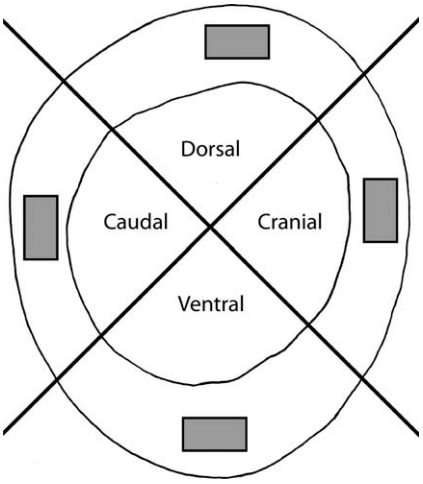

Fig. 2. Schematic midshaft cross-section to illustrate sampling strategy within a given element. The section was divided into four quadrants: dorsal, cranial, ventral, caudal. A 0.5 × 1.0 mm area was used for sampling each of the four quadrants.

Plexiglass Acrylic slide (Professional Plastics) using Clear Weld 2-ton epoxy (Devcon). Each specimen was ground to a thickness of ~ 100 μm and polished using a series of CarbiMet®/MicroCut® abrasive grinding papers (grit values 320, 600, and P4000, Buehler) on a Buehler MetaServ® 2000 Variable Speed Grinder-Polisher. Polishing was completed with MicroPolish® II 1.0 micron deagglomerated alumina suspension and a felt polishing pad (Buehler). The section thickness was monitored during grinding using a Mitutuyo ± 0.01 mm micrometer.

Vascular Organization

A series of images was taken from each specimen at 40× magnification using a Nikon DMX 1200 digital camera attached to a light microscope (Nikon Labophot-2). The images were reassembled using AutoPano Pro (v1.3.0) to create a composite image of each specimen. Each cross section was divided into four quadrants: dorsal, cranial, ventral, and caudal. A 0.5 × 1.0 mm^2 area was sampled within each quadrant midway between the endosteal and periosteal borders (Fig. 2). The primary vascular canals in each sample were classified following de Margerie (2002) into one of the following categories: longitudinal, radial, circular, or oblique (Fig. 1). The number of each type of canal was tallied and the Laminarity Index was calculated (LI = total # circular canals/total # canals). The LI was calculated for each of the four quadrants in each of the three main wing bones (Table 1, Supplementary Information). A quadrant homogeneity test was performed on one specimen (albatross humerus, OUVC 10225), in which nine 0.5 × 1.0 mm^2 samples were taken within a single quadrant. The sample selected for this study was within one standard deviation from the mean LI of all samples. Although other methods have been developed for characterizing vascular canal organization in bone (e.g., see de Boef and Larsson, 2007; Lee, 2007), we have purposefully elected to employ the system developed by de Margerie (2002). Not only does this allow us to directly compare our data with published laminarity indices (de Margerie 2002; de Margerie et al., 2005), but it provides an explicit test of the relationship between LI and inferred loading patterns (e.g., resistance to torsion). Whereas only primary structure was classified, the presence of secondary (Haversian) osteons in each quadrant was noted. LI values were Arcsine transformed for normality (Zar, 1999). A nested analysis of variance with multiple comparisons was used to test for differences at the following levels: among quadrants (within each element), among elements (within each species), and among species/flight mode.

RESULTS

The LI for all species sampled ranged from 0 (no circular canals) to 0.83 (over 80% circular canals) (Table 1). Figure 3 illustrates example cross-sections of all three elements to show the range in vascular canal organization. A nested ANOVA indicates significant differences among quadrants within each element ($P = 0.05$), no difference among elements within each species/flight mode ($P = 0.099$), and significant difference between species/flight mode ($P < 0.0001$). Among quadrants, the dorsal quadrant was significantly more laminar than the ventral quadrant, but only in the humeri and not the two more distal elements (Fig. 4). Among flight modes, the flapping and static soaring birds exhibited significantly more laminar wing elements than the dynamic soaring bird (Fig. 5). As the dynamic soaring group did not meet the assumption of normality, even after Arcsine transformation, a nonparametric Kruskal-Wallis test confirms there is a significant difference in laminarity among flight modes ($P < 0.0001$).

de Margerie quantified all primary vascular canals in the entire section in his 2002 study. A post-hoc analysis of three individuals included in this study (albatross CMC, OUVC 10225; pelican CMC, OUVC 10430; cormorant CMC, OUVC 10431) indicates that the quadrant samples taken here are a good approximation of the overall LI. The LI calculated from the entire CMC section of the albatross (OUVC 10225) was 0.062, compared with 0.07 calculated from the quadrant samples. Similarly, for the entire CMC of the pelican (OUVC 10430) the LI was 0.37 compared with 0.39 from the quadrant samples and for the cormorant (OUVC 10431) the LI from the entire CMC was 0.19 compared with 0.16 from the quadrant samples.

Remodeling of Avian Cortical Bone

Secondary (Haversian) remodeling was noted in several of the specimens examined (Fig. 6; Table 1). Secondary osteons were surrounded by a cement sheath, clearly cut across primary bone structure, were generally oriented longitudinally, and were typically located along the endosteal surface. Regarding humeri, remodeling was noted in only two cormorants (occurring in the dorsal quadrant and cranial quadrant) and six albatross specimens, the latter of which appear to have no regular pattern of remodeling as all quadrants are represented. Remodeling was noted in the ulnae of one cormorant (dorsal quadrant), one pelican (ventral quadrant), and four albatross specimens (all quadrants represented). Remodeling was noted in the CMC of four cormorants (dorsal, cranial, and ventral quadrants), two pelicans (dorsal quadrant), and six albatross specimens (all quadrants represented, see Table 1). When present along the

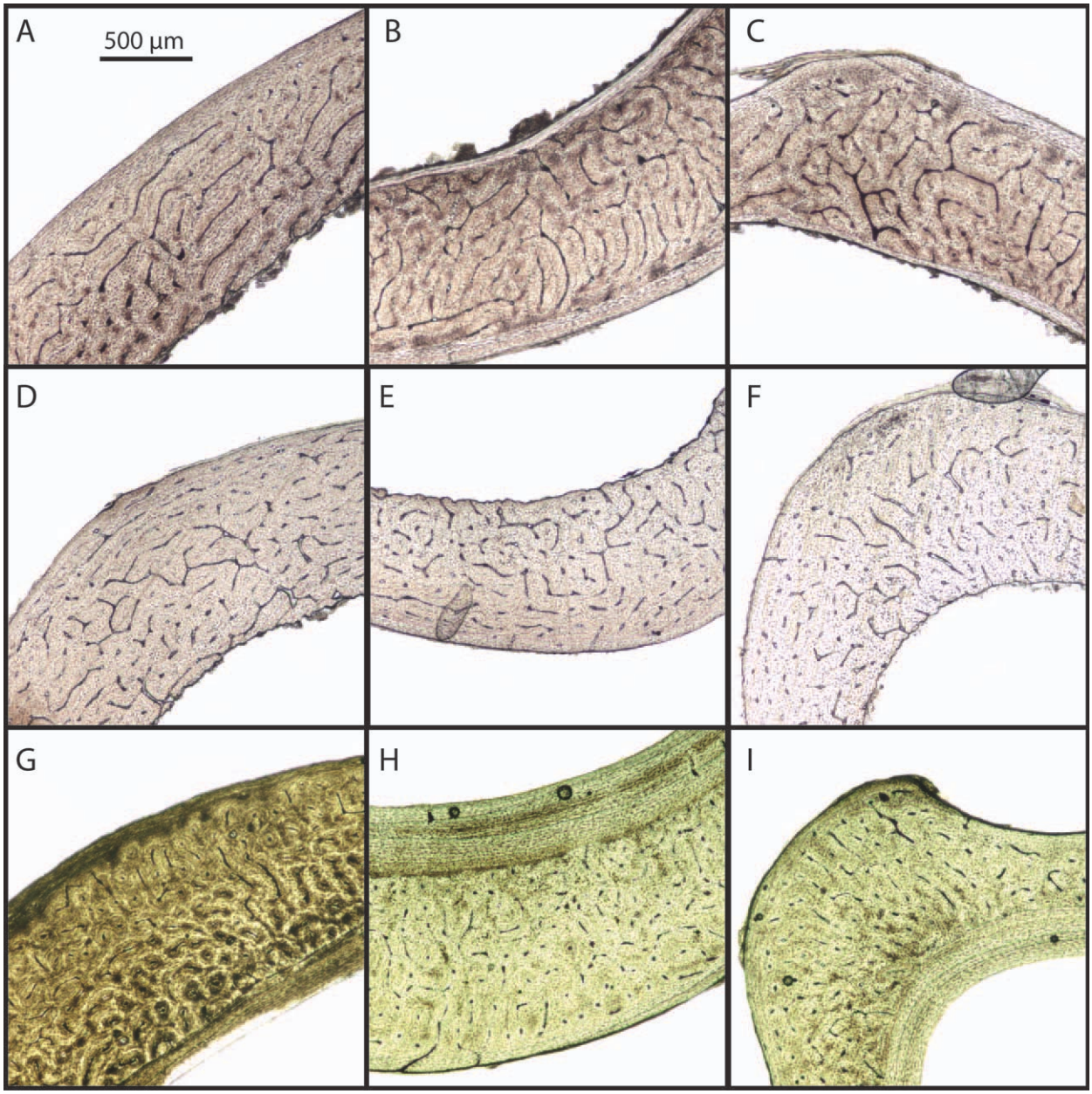

Fig. 3. Example histology sections of humeri (**A, D, G**), ulnae (**B, E, H**), and carpometacarpi (**C, F, I**) of the Brown pelican (*Pelecanus occidentalis*, OUVC 10430) (**A, B, C**), double-crested cormorant (*Phalacrocorax auritus,* OUVC 10431) (**D, E, F**), and Laysan albatross (*Phoebastria immutabilis*, OUVC 10480) (**G, H, I**) exhibiting a range of primary vascular canal orientations.

periosteal margin, secondary osteons were restricted to the dorsal quadrant of the CMC and were identified in four cormorants, two pelicans, and four albatross specimens.

DISCUSSION

Evidence of Bone Functional Adaptation in Wing Element Microstructure

An initial prediction of this study was that the Laminarity Index (LI) as described by de Margerie (2002) would vary among quadrants at least within the ulna and carpometacarpus (CMC) due to the localized loads placed on these elements by the attachment of the secondary and primary flight feathers. We expected these elements to exhibit a high LI in the "compression" area and low LI in the "tension" and neutral axis areas, similar to that found in an examination of turkey ulnae by Skedros and Hunt (2004). The presence of local differences in microstructure in response to specific loads, as found by Skedros and Hunt (2004) would suggest the presence of bone functional adaptation during the life of the organism. However, the results of this study indicate very few differences in primary vascular canal

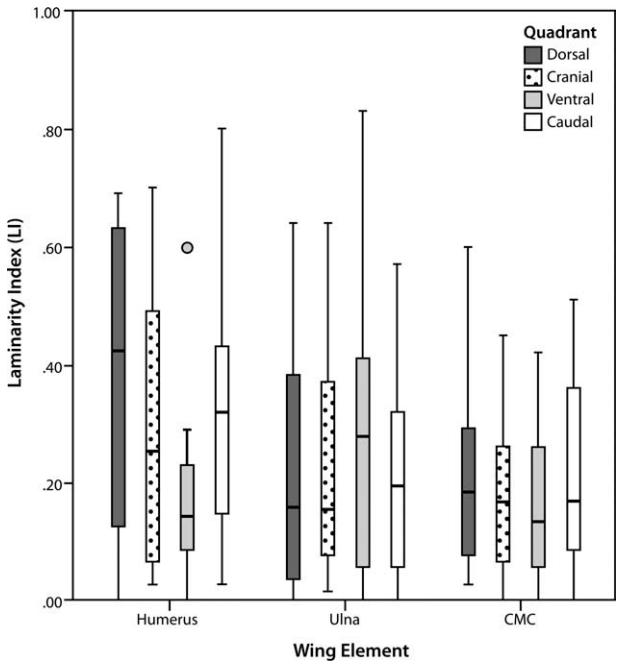

Fig. 4. Arcsin transformed Laminarity indices (LI) by quadrant within the three wing elements for the focal species examined in this study. A significant difference was detected between the dorsal and ventral quadrant in the humerus only ($P = 0.05$). Circle indicates statistical outlier.

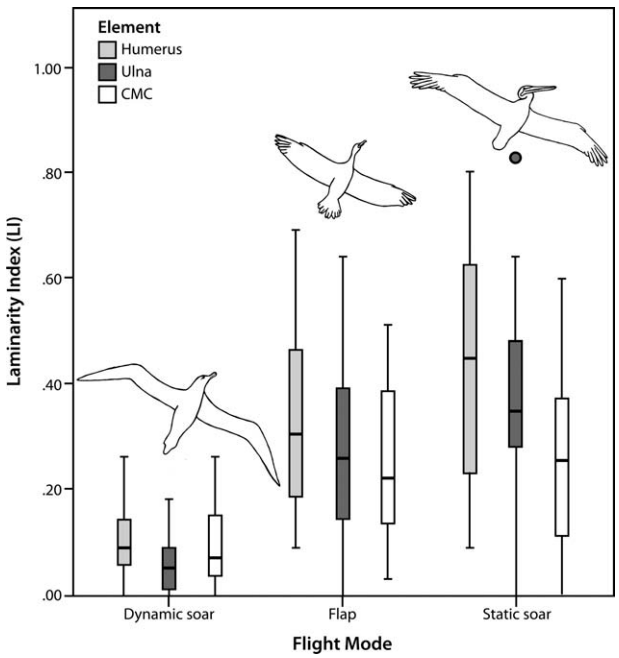

Fig. 5. Arcsin transformed Laminarity indices (LI) for individual bones of the three focal species examined in this study. No significant differences were detected among the three main wing elements within any of the three species examined ($P = 0.099$). However, significant differences were detected in LI among the three species. The dynamic soaring group (albatross) exhibited significantly lower LI than the flapping (cormorant) and static soaring (pelican) group ($P < 0.0001$). Circle indicates statistical outlier.

orientation among the quadrants within each of the three main wing elements in the species examined (Fig. 4). A significant difference does exist between the dorsal and ventral quadrants in the humerus, possibly to accommodate the "compression" and "tension" regions of the cross section during bending loads. However, no significant differences in the LI among the quadrants were found in the ulna or CMC, elements that are hypothetically experiencing equal or more frequent bending loads than the humerus. Thus, results of this study do not support the general concept that primary vascular canal organization within a given quadrant of a wing elements is reflective of bone functional adaptation (although see below regarding the periosteal distribution of secondary osteons).

The humerus of pelecaniform birds has been found to exhibit a shape predicted to be more resistant to torsional loads (high polar moment of area standardized to length of the element) than the ulna or CMC (Simons et al., 2011). If high laminarity is an adaptation to resist torsional load (as hypothesized by de Margerie, 2002; de Margerie et al., 2005), then the humerus of the birds examined should exhibit higher LI than the ulna or CMC. This prediction was not supported by the results of this study. In fact, there were no statistical differences among the three elements for any of the species examined (Fig. 5). It is possible, however, that an increased sample size could change this result. As it stands, even though the overall cross-sectional shape is different among elements, with the CMC exhibiting a more elliptical shape and the humerus exhibiting a more circular shape (Simons et al., 2011), the primary vascular canal orientation remains the same. This suggests that whereas the cross-sectional shape may be responding (over evolutionary time) to the loads placed on different elements, the microstructure may be strictly genetically determined and seems be constrained within a species (Enlow, 1968; Currey, 2002; de Margerie et al. 2006).

Evolution of Microstructure in Response to Flight Mode

Although no differences were found among the elements within a species, significant differences were found among species that exhibit different primary flight modes (Fig. 5). The dynamic soaring albatross exhibited a significantly lower LI in all three elements than the static soaring pelican and the continuous flapping cormorant. The differences in laminarity observed among these three species could be attributed to several factors: difference in wing biomechanics/loading (wing shape and flight mode), phylogeny, or ontogeny (particularly differential growth of the wing). First, several differences in overall wing morphology and the general ecology of these animals may help to explain this relationship. An apparent difference between albatrosses and the two pelecaniforms (cormorants and pelicans) is where they live and how they obtain food. Albatrosses are highly marine birds that forage for food over the open ocean (Tickell, 2000). Cormorants and pelicans, however, are near-shore species that tend to forage in shallow water (Nelson, 2005). More pertinent to this discussion,

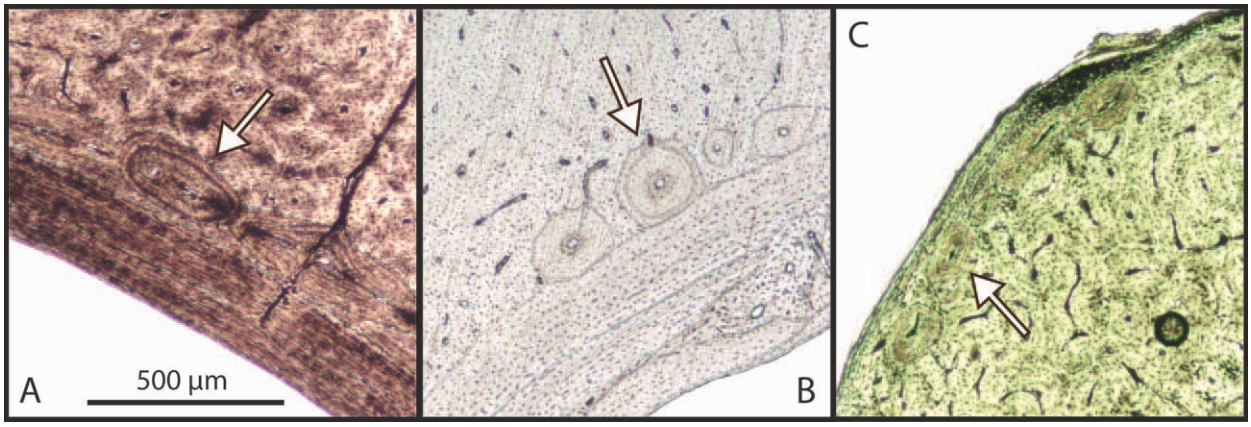

Fig. 6. Example sections showing secondary (Haversian) osteonal remodeling of avian cortical bone in the (**A**) humerus of a Laysan albatross (*Phoebastria immutabilis*, OUVC 10483), (**B**) ulna of a Laysan albatross (*Phoebastria immutabilis*, OUVC 10225), and (**C**) carpometacarpus of a Double-crested cormorant (*Phalacrocorax auritus*, OUVC 10479). Arrows indicate example secondary osteons.

however, is that pelicans and cormorants both exhibit wings that are broad relative to their body size (i.e., they exhibit a relatively long chord length). The secondary flight feathers (i.e., those attached to the ulna) make up the width of the wing, and these long feathers act as lever arms creating torsional loads on the ulna, specifically, and likely the entire wing skeleton (Simons et al., 2011). In contrast, the long slender wing of the albatross is modeled to be experiencing primarily bending loads. Whereas the pelican and cormorant utilize different primary flight modes, when differences in body size are controlled for, there are many similarities in wing and wing element morphology (Simons, 2010). A multivariate analysis of the external shape of the wing elements revealed that these two genera were closer to each other than to other pelecaniforms sampled in morphological multivariate space and in fact overlapped completely on one axis.

The differences in LI among birds with different whole wing shapes are consistent with the results of de Margerie et al. (2005). In that study, the authors evaluated microstructure of limb elements in a wide range of birds. In general, they found that birds with a broad wing shape such as buzzards, hawks, cormorants, and pheasants had humeri and ulnae exhibiting high LI. In contrast, birds with long slender wings, such as albatrosses and petrels exhibited low LI in the wing elements. To examine this relationship further and also to begin to investigate the potential role of phylogeny, we sampled the humeri from two additional species (N = 2 for each species). The Northern gannet (*Morus bassanus*) is a pelecaniform and therefore closely related to the pelican and cormorant, but exhibits a long slender wing and utilizes dynamic soaring similar to the albatross. The Red-tailed hawk (*Buteo jamaicensis*), a falconiform, is distantly related to all species in the study, but exhibits a short broad wing and utilizes static soaring. The gannet exhibits low LI similar to the albatross and the hawk exhibits high LI similar to the pelican (Fig. 7), suggesting that whole wing shape (shown to be highly correlated to flight mode; Savile, 1957; Warham, 1977; Norberg, 1985; Norberg, 1995; Brewer and Hertel, 2007) rather than phylogenetic relationships may be determining the microstructure of wing elements. The preliminary results offered by the inclusion of additional taxa help bolster a functional relationship between wing shape/flight mode variables and LI, but a broader sample is required to fully investigate any role that phylogeny may play in dictating bone microstructure.

The LI assesses the degree of circular canals in a section, but it does not quantify the proportion of other types of canal organization (longitudinal, radial, oblique). Given that experimental data (Swartz et al., 1992; Biewener and Dial, 1995) have demonstrated that torsion and bending appear to be the dominant loading regimes on the humerus during flight, this study was developed around characterizing that morphology hypothesized to be directly related to torsion resistance (de Margerie 2002, de Margerie et al., 2005), thus LI was the chosen metric. However, future work may explore methods that fully characterize all potential canal orientations (i.e., radial, oblique, longitudinal and circular) (de Boef and Larsson, 2007; Lee, 2007).

Implications of Growth Dynamics For Bone Microstructure

In addition to the functional loading environment, there is evidence suggesting that the degree of laminarity is correlated with the bone growth rate of the element, with higher laminarity being the result of slower bone growth rates (de Margerie et al., 2004). Specific bone growth rates of the wing elements of these three species are unknown. Other growth parameters, however, do not seem to correlate with the laminarity measures found in this study. For example, all three species are classified as altricial birds and therefore experience relatively rapid growth after hatching (Ricklefs, 1968; Ricklefs, 1973). The growth rate (K_G), defined as growth in body weight, for the cormorant is $K_G = 0.133$ (fastest of the three species), for the pelican is $K_G = 0.071$, and for the albatross is $K_G = 0.016$ (slowest of the three species; Ricklefs, 1973). Concordantly,

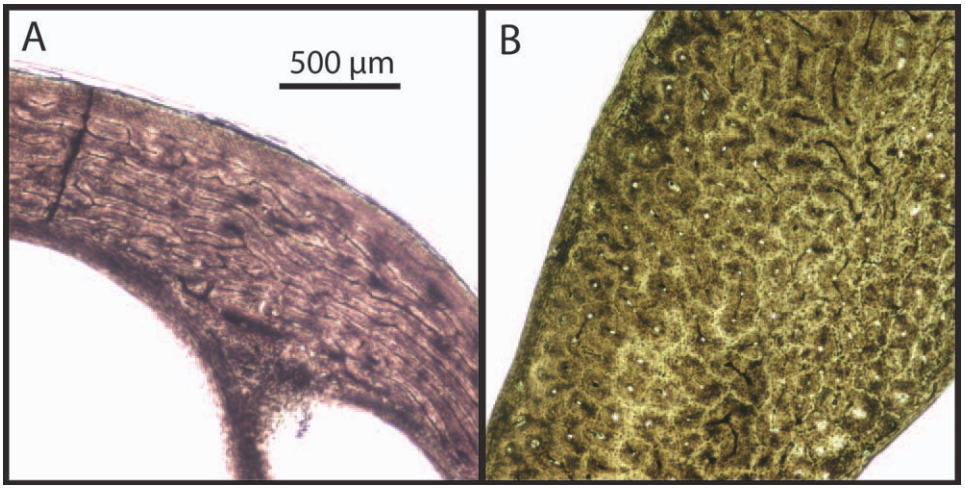

Fig. 7. Example sections of humeri of (**A**) the static soaring Red-tailed hawk (*Buteo jamaicensis*, OUVC 10506) and (**B**) the dynamic soaring Northern gannet (*Morus bassanus*, OUVC 10434).

albatross chicks take longer to fledge (165 days) than the cormorant (42–49 days) or pelican (80 days; Ricklefs, 1973). For overall body growth, at least, these species do not support the hypothesis that higher laminarity is the result of slower growth rate. Wing elements, however, have been shown in at least one species, to grow at a different rate (with positive allometry) in relation to body mass (Carrier and Leon, 1990). In the semiprecocial California gull, the wing element lengths, midshaft diameters, and second moments of area all increased rapidly, with positive allometry, throughout the entire growth period until adult size was reached (Carrier and Leon, 1990). Also, growth rates of elements are not always constant. For example, the ulna of Double-crested cormorants grows slowly in the first week after hatching and then more rapidly (Dunn, 1975). Finally, it is also unclear to what degree chicks of the different species load the forelimb skeleton during the immediate post-hatch (but long before actual flight loads are experienced) period and what impact this may have on the developing wing bones. Without specific data on individual bone growth rates for these species (i.e. by using bone labeling techniques), we cannot support or refute the hypothesis that primary vascular canal orientation correlates with bone growth.

Haversian Remodeling in Wing Elements

In general the bone tissue of the wing elements in this study was predominantly primary in nature. However, small areas of localized secondary osteonal remodeling were identified (Fig. 6; Table 1). All examined albatross specimens exhibited some remodeling in all three elements, remodeling was variably present in the cormorant, and almost no remodeling was identified in the pelican. Secondary remodeling of primary bone structure is generally thought to serve one of two main functions: removing damaged bone tissue that accrues with age of the individual, and restricting the propagation of microcracks (Currey, 2002). Remodeling was identified consistently in all elements of albatross, but found predominantly in the CMC of the cormorant. It is possible that the remodeling may have a function related to repairing microcracks that occur during physiologic loading (Reilly and Currey, 1999). The CMC of the cormorant is experiencing high frequency loading during continuous flapping that may preferentially cause microcracks and stimulate remodeling. In addition, albatrosses use high velocity ocean winds for dynamic soaring and thus all wing elements may be under more stress. It is just as likely, however, that the presence of secondary osteonal remodeling reflects the age of the individuals. Although all specimens included in this study were adults, the specific ages of the individuals were unknown. The albatross in this study is a long lived species, with some individuals recorded as reaching 40 years of age (Fisher, 1975). In contrast, individuals of this species of cormorant have a lifespan of about 15 years (Nelson, 2005). The Brown pelican has also been known to reach 30–40 years of age. However, fewer than 2% of individuals live more than 10 years (Nelson, 2005), suggesting our sample may have consisted of young adult specimens.

The CMC was the most consistently remodeled element (12 out of 18 individuals). In addition, 10 of these individuals exhibited secondary osteonal remodeling on the periosteal surface exclusively within the dorsal quadrant (Fig. 6C). It is likely that the localized loads caused by the attachment of the primary feathers are stimulating remodeling in this quadrant. So whereas there is no evidence that the load induced by the primary flight feathers causes functional adaptation of the primary structure, it may be stimulating secondary osteonal remodeling on the periosteal surface. The pattern of secondary remodeling in this sample of birds provides an interesting avenue for further study. Future studies of secondary osteons in birds could employ quantitative approaches similar to that of MacFarlin et al. (2008).

CONCLUSION

In this study we collected data on the degree of primary vascular canal laminarity (i.e., the proportion of

circularly orientation of vascular canal networks) from the three main wing elements in three species of birds that utilize different primary flight modes: the Double-crested cormorant, a continuous flapper; the Brown pelican, a static soarer; and the Laysan albatross, a dynamic soarer. We addressed three main hypotheses based on previous studies of (1) wing bone microstructure, (2) cross-sectional geometry, and (3) known or inferred biomechanical loading of the wing, namely that there would be differences in the degree of laminarity among the main quadrants of each element, among the three wing elements, and among birds that utilize different primary flight modes. None of our predictions were supported in the way we expected. Almost no differences in laminarity among the four quadrants were identified within the species examined. Moreover, no significant differences were identified among the three elements within a given species. These results, therefore, do not support the concept of bone functional adaptation in the primary vascular structure of the wing elements within the lifetime of the examined individuals. Significant differences in laminarity were identified among the three primary flight modes, with both flapping and static soaring birds exhibiting significantly higher laminarity than the dynamic soaring birds. This pattern may be explained by the difference in overall wing shape: whereas dynamic soaring birds have long slender wings, flappers, and static soaring birds have broader wings with a larger wing chord that would necessarily impart a higher torsional moment on the feather-bearing wing bones. The presence of secondary osteonal remodeling on the periosteal surface exclusively within the carpometacarpus suggests that primary flight feathers induce a localized load on that element, but that such loading stimulates remodeling rather than functional adaptation of the primary structure. Additional research is necessary to resolve how factors such as growth dynamics and phylogeny may impact bone microstructural organization and its potential for establishing biomechanical loading-resistance relationships in the avian forelimb skeleton.

ACKNOWLEDGEMENTS

The authors thank R. Hikida, T. Hieronymus, S. Williams, and A. Lee for assistance with histological preparation and analysis. They also thank W. and B. Fox (Pelican Harbor Seabird Station, Miami, FL), C. Rehkemper and B. Zaun (Kauai National Wildlife Refuge Complex, HI), and W. Roosenburg for salvage specimens used during the course of this work.

LITERATURE CITED

Amprino R. 1947. La structure du tissu osseux envisagée comme expression de différences dans la vitesse de l'accroissement. Arch Biol (Liege) 58:315–330.

An YH, Martin KL, editors. 2003. Handbook of histology methods for bone and cartilage. Totowa, New Jersey: Humana Press.

Beer FB, Johnston ER, DeWolf JT. 2006. Mechanics of materials. New York: McGraw Hill Co.

Biewener AA, Dial KP. 1995. In vivo strain in the humerus of pigeons (*Columba livia*) during flight. J Morphol 225:61–75.

Brewer ML, Hertel F. 2007. Wing morphology and flight behavior of pelecaniform seabirds. J Morphol 268:866–877.

Carrier D, Leon LR. 1990. Skeletal growth and function in the california gull *Larus californicus*. J Zool (London) 222:375–390.

Castanet J, Currey-Rogers K, Cubo J, Boisard J-J. 2000. Periosteal bone growth rates in extant ratites (ostriche and emu). Implications for assessing growth in dinosaurs. CR Acad Sci Paris, Sci. la Vie 323:543–550.

Currey JD. 1960. Differences in the blood-supply of bone of different Histological types. J Microscopical Sci 101:351–370.

Currey JD. 2002. Bones: structure and mechanics. Princeton, NJ: Princeton University Press.

de Boef M, Larsson HCE. 2007. Bone microstructure: quantifying bone vascular orientation. Can J Zool 85:63–70.

de Margerie E. 2002. Laminar bone as an adaptation torsional loads in flapping flight. J Anatomy 201:521–526.

de Margerie E, Cubo J, Castanet J. 2002. Bone typology and growth rate: testing and quantifying Amprino's rule' in the mallard (*Anas platyrhynchos*). Comptes Rendus Biologies 325:221–230.

de Margerie E, Robin J-P, Verrier D, Cubo J, Groscolas R, Castanet J. 2004. Assessing a relationship between bone microstructure and growth rate: a fluorescent labelling study in the king penguin chick (*Aptenodytes patagonicus*). J Exp Biol 207: 869–879.

de Margerie E, Sanchez S, Cubo J, Castanet J. 2005. Torsional resistance as a principal component of the structural design of long bones: comparative multivariate evidence in birds. Anatomical Record Part A 282:49–66.

de Margerie E, Tafforeau P, Rakotomanana L. 2006. In silico evolution of functional morphology: a test on bone tissue biomechanics. J R Soc Interface 3:679–687.

de Ricqlés P, Meunier FJ, Castanet J, Francillon-Vieillot H. 1991. Comparative microstructure of bone. In: Hall BK, editor. Bone, Vol. 3: Bone matrix and bone specific products. Boston, MA: CRC Press. p 1–78.

Dunn EH. 1975. Growth, body components and energy content of nestling Double-crested cormorants. Condor 77:431–438.

Enlow DH. 1968. Wolff's law and the factor of architectonic circumstance. Am J Orthodontics 54:803–822.

Enlow DH, Brown SO. 1957. A comparative histological study of fossil and recent bone tissue. Part II. Texas J Sci 9:186–214.

Fisher HI. 1975. Longevity of the Laysan albatross, *Diomedea immutabilis*. Bird-Banding 46:1–100.

Johnsgard PA. 1993. Cormorants, darters, and pelicans of the world. Washington: Smithsonian Institution Press.

Lee AH. 2007. Interplay between growth and mechanics in the evolution of bone microstructure in dinosaurs. PhD dissertation. University of California, Berkeley. 210 pp.

McFarlin SC, Terranova CJ, Zihlman AL, Enlow DH, Bromage TG. 2008. Regional variability in secondary remodeling within long bone cortices of catarrhine primates: the influence of bone growth history. J Anatomy 213:308–324.

Nelson JB. 2005. Pelicans, cormorants, and their relatives: the pelecaniformes. New York: Oxford University Press.

Norberg UM. 1985. Flying, gliding, and soaring. In: Hildebrand M, Bramble DM, Liem KF, Wake DB, editors. Functional vertebrate morphology. Cambridge, MA: Harvard University Press. p 129–158.

Norberg UM. 1995. Wing design and migratory flight. Israel J Zool 41:297–305.

Pennycuick CT. 1967. The strength of the Pigeon's wing bones in relation to their function. J Exp Biol 46:219–233.

Reilly GC, Currey JD. 1999. The development of microcracking and failure in bone depends on the loading mode to which it is adapted. J Exp Biol 202:543–552.

Ricklefs RE. 1968. Patterns of growth in birds. The IBIS 110: 419–451.

Ricklefs RE. 1973. Patterns of growth in birds. II. Growth rate and mode of development. IBIS 115:177–201.

Savile DBO. 1957. Adaptive evolution in the avian wing. Evolution 11:212–224.

Simons ELR. 2010. Forelimb skeletal morphology and flight mode evolution in pelecaniform birds. Zoology 113:39–46.

Simons ELR, Hieronymus, TL, O'Connor PM. 2011. Cross-sectional geometry of the forelimb skeleton and flight mode in pelecaniform birds. J Morphol 272:958–971.

Skedros JG, Hunt KJ. 2004. Does the degree of laminarity correlate with site-specific differences in collagen fibre orientation in primary bone? An evaluation in the turkey ulna diaphysis. J Anat 205:121–134.

Skedros JG, Hunt KJ, Hughes PE, Winet H. 2003. Ontogenetic and regional morphologic variations in the turkey ulna diaphysis: implications for functional adaptation of cortical bone.Anat Record Part A: Discov Mol Cell Evol Biol A 273:609–629.

Starck JM, Chinsamy A. 2002. Bone microstructure and developmental plasticity in birds and other dinosaurs. J Morphol 254:232–246.

Swartz SM, Bennett MB, Carrier DR. 1992. Wing bone stresses in free flying bats and the evolution of skeletal design for flight. Nature 359:726–729.

Tickell WLN. 2000. Albatrosses. New Haven: Yale University Press.

Warham J. 1977. Wing loadings, wing shapes, and flight capabilities of Procellariiformes. New Zealand J Zool 4:73–83.

Wolff J. 1892. Das gesetz der transformation der knochen. A. Hirshwald, Berlin.

Zar JH. 1999. Biostatistical analysis. 4th ed. Upper Saddle River, New Jersey: Simon & Shuster.